



Evolution of microstructure and texture during cold rolling and high-temperature annealing in Ni–5 at% W substrate for coated conductor

Xing-Pin Chen* , Dan Chen, Hong-Fu Sun, Li-Xia Wang, Du Shang

Received: 7 December 2016 / Revised: 20 February 2017 / Accepted: 1 March 2018 / Published online: 2 April 2018
© The Nonferrous Metals Society of China and Springer-Verlag GmbH Germany, part of Springer Nature 2018

Abstract The evolution of microstructure and texture at four strain levels was investigated in Ni–5 at% W alloy by means of electron backscatter diffraction (EBSD) technique. The deformation microstructure evolves gradually from microbands (MBs) to typical lamellar structures with strain increasing in cold-rolled materials, while only lamellar structures in heavily cold-rolled materials. Subsequently, quantitative analysis of microstructure and texture was performed. It indicates that the texture is a typical pure metal deformation texture, but a few cube and rolling direction (RD)-rotated cube orientations also can be observed in the deformed samples. The use of high-temperature annealing enables an area fraction of cube orientation > 95% to be obtained for high strained substrate. In addition, it is worth noting that the point-to-point misorientation inside the band with various orientations is found to keep quite low. But the point-to-origin misorientation over the same distance is dependent on strain and orientation type in the band. The cube-oriented regions were characterized by a high accumulated orientation gradient, close to 28°, compared to the non-cube-oriented regions. This means that the accumulated orientation gradient only occurs in the cube band with the reduction of 98%, which partly explains the formation of strong cube texture after high-temperature annealing.

Keywords Cold rolling; Microstructure; Texture; Orientation relationship

1 Introduction

The second-generation coated superconductor has been the research focus for many years, among which YBa₂Cu₃O_{7-δ} (YBCO) coated conductor attracted the most attention for its high irreversible field and ability to maintain high critical current density under high magnetic field. Compared with the powder metallurgy process used to manufacture bismuth strontium calcium copper oxide (BSCCO), YBCO coated conductors is a multilayer coating on a specialized metal substrate, and the associated techniques are referred to as “coated conductor technology.” The rolling assisted biaxially textured substrates (RABiTS™) method [1–3], which has been developed at ORNL, USA, is probably the most cost-effective approach for the production of long lengths of high-temperature superconducting (HTS) YBCO tapes.

Ni–5 at% W (Ni–5W) alloy is widely used as metallic substrate for the coated-conductor technology. In order to achieve a strong cube texture, the effects of rolling reduction and annealing temperature on the microstructure and texture evolution in nickel and Ni–W alloys have been discussed by several groups [4, 5]. Moreover, for improving the mechanical properties and suppressing ferromagnetism, increasing W content in Ni–W substrates (which can dissolve and form solid solutions) is an effective approach [6, 7]. However, when the addition of alloy element W exceeds 5 at%, the stacking fault energy of Ni–W alloy decreases distinctly, thus leading to a weak cube texture after recrystallization [8]. Recently, Zhao et al. [9] have demonstrated that the dominant recrystallization cube texture in Ni–7 at% W tapes has been developed through an advanced sintering technique. In addition, a specific intermediate annealing in the cold rolling process has been

X.-P. Chen*, D. Chen, H.-F. Sun, L.-X. Wang, D. Shang
College of Materials Science and Engineering, Chongqing University, Chongqing 400044, China
e-mail: xpchen@cqu.edu.cn

introduced to improve the sharpness of cube texture in Ni–7.5 at% W [10].

Commonly, transmission electron microscopy (TEM) was the main method used by most researchers for characterizing heavily rolled alloys over the past few decades [11–13]. The specimens observed in TEM are relatively small, and the areas selected for examination are random. Therefore, it is difficult to judge whether the results are representative for a general observation on the grain scale. Within a general framework, the most important microstructural features of deformation materials are the low-angle and high-angle grain boundaries. These can usually be characterized and quantified much more efficiently using a field emission gun scanning electron microscope (FEGSEM) equipped with a high-resolution electron backscattered diffraction (EBSD) detector, and this technique is becoming the main tool of the present investigation.

In previous studies [14–16], much work has already been carried out on the optimization of the thermo-mechanical processing to realize a strong cube texture. The exact phenomena involved in the development of a strong cube texture in the recrystallized Ni–5W alloy, however, are still controversial. In the present work, a series of Ni–5W alloy substrates were cold-rolled to different thickness reductions and subsequently annealed at high temperature. The effect of cold rolling reduction on microstructure and texture evolution was investigated systematically. And the reason why cube orientation is preferred over the other orientation during annealing process was discussed.

2 Experimental

The power metallurgy (PM) route was employed to prepare the initial Ni–W ingot. The nickel power with purities of 99.99% and tungsten power with purities of 99.9% were weighted according to the stoichiometric ratio of Ni–5W followed by sintering of the green compacts in flowing H₂ atmosphere. Homogeneous alloying between Ni and W was established during the sintering stage. The sintered compact was subsequently hot-forged at 1200 °C to form plates with about 30 mm in thickness. Then, the plates were hot-rolled to about 10 mm followed by cold rolling to 4 mm in thickness. At this stage, an intermediate annealing (800 °C for 1 h) was done to develop a fine grain and be prepared for the further cold rolling. The annealing strips were further cold-rolled in several passes with an average of 5% cold reduction per rolling pass. At last, four strain levels of substrates were produced. The final thicknesses reductions of the tapes are 61%, 77%, 89% and 98%, corresponding to a von Mises strain (ε_{VM}) of 1.09, 1.70, 2.54, and 4.52, respectively.

The microstructure and texture were examined in the longitudinal section bounded by the normal direction (ND)–rolling direction (RD) using a Channel 5 EBSD analysis system attached to a FEI Nova 400 Nano scanning electron microscope (SEM), adopting an accelerating voltage of 20 kV with a working distance of 15 mm and a 70° sample tilt angle. The samples which would be investigated were prepared by mechanical polishing to SiC4000 followed by electro-polishing using a mixed solution at ~ 0 °C and 15 V for 45 s (the volume ratio of the polishing solution is HClO₄:C₂H₅COOH:C₂H₅OH = 1:3:4). The step size of the EBSD maps was 1 μm for the fully recrystallized tapes (map size 400 μm × 400 μm). For the cold-rolled tapes, a step size of 100 nm was chosen. The EBSD data were used to reconstruct orientation image maps (OIM). Considering the limited angular resolution of the EBSD technique [17], in this paper, a critical misorientation angle of 2° was applied to observe boundaries in the orientation maps. The low-angle grain boundaries (LAGBs) are defined as misorientations in the range of 2°–15° and are represented by thin gray lines, and the high-angle grain boundaries (HAGBs) are defined as misorientations more than 15° and are shown by thick black lines. Texture components are defined within a 15° deviation from the ideal orientations. The texture components considered include typical rolling texture such as copper ($\{112\} \langle 111 \rangle$), S ($\{123\} \langle 634 \rangle$), brass ($\{110\} \langle 112 \rangle$) and a small number of cube ($\{001\} \langle 100 \rangle$) and Goss ($\{011\} \langle 100 \rangle$). The remaining texture are grouped together and referred to as “other.”

To estimate the strength of the tapes in various strains, Vickers microhardness measurements were taken using loads of 2.94 N with a dwell time of 15 s. In order to ensure the statistical analysis, five indentations were taken for each sample in different areas.

3 Results

3.1 Overview of microhardness and microstructure with strain increasing

The main purpose of this investigation is to study the evolution of microstructure during moderate and large rolling deformation. Extensive previous studies have demonstrated that the largely deformed and subsequently annealed process at high temperature would form sharp cube texture in nickel alloy [18–20]. The detailed descriptions of the microstructure developed from moderate to large strains will be exhibited, and more attention would be paid to the effects of strains on the various parameters of deformed microstructure.

The microhardness curve for samples with various strains is shown in Fig. 1. It is clear that the hardness gradually changes with strain increasing. After a total reduction of 61% ($\varepsilon_{vM} = 1.09$), the hardness of the sample reaches about HV 350, which is about three times higher than that of hot-rolled samples. And afterward, the microhardness of Ni–W alloy increases with the deformation strains increasing from a ε_{vM} of 1.09–4.52. The increase in hardness resulting from the work hardening has a close relationship with dislocation density in deformed metal materials.

The crystal orientation maps of typical lamellar regions from various deformations are shown in Figs. 2 and 3. According to these maps, the deformation microstructures of microbands have an uneven distribution along the rolling direction, and the orientation bands gradually become smaller as the strain increases. In addition, there is an obvious characteristic of localized glide band which shows an angle of 30° to the RD in the longitudinal side plane. Figure 3a, c, e, following 77%, 89% and 98% cold rolling, respectively, shows that the microstructure at large strain is characterized by typical lamellar structure subdivided by HAGBs along ND. As the strain increases, the lamellar structure becomes thinner and the boundaries are dominantly composed of lamellar boundaries (LBs). At 98% reduction, the localized glide bands are no longer seen in the EBSD maps and the lamellar structure is parallel to rolling direction. Similar microstructures of cold-rolled metal alloys have been reported in the relevant literature [21].

3.2 Quantitative microstructure

The improvement of high-resolution EBSD in FEGSEM enables the detailed quantitative analysis possible. Various microstructural information such as the content of high-angle boundaries and the spacing of geometrically

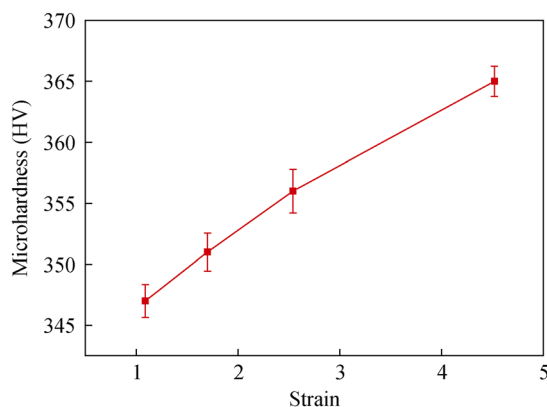


Fig. 1 Evolution of microhardness for different reduction in Ni–W substrates

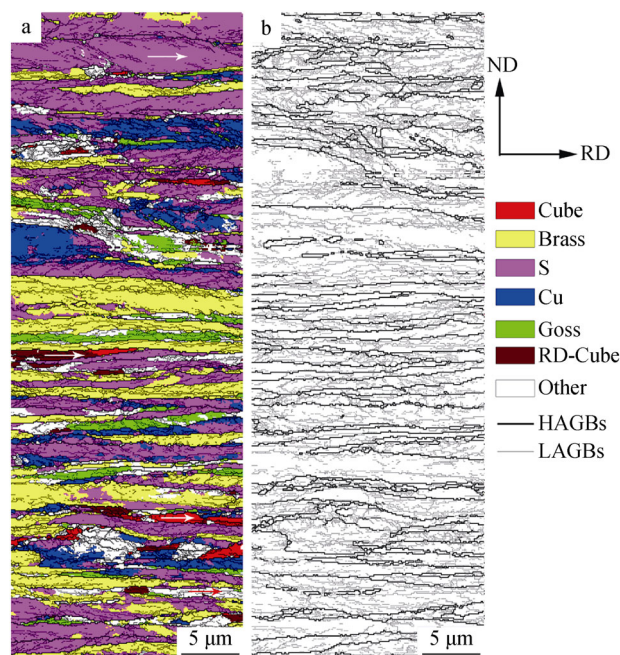


Fig. 2 EBSD maps of Ni–W substrates with 61% rolling reduction: **a** OIM and **b** grain boundary map

necessary boundaries (GNBs) as a function of strains could be extracted from EBSD maps.

In Fig. 4, grain boundary character distributions for various strains are presented. Most of the grain boundaries are low-angle boundaries for all of the four strain levels from 61% to 98%. With the increase in reduction, the content of HAGBs tends to increase from 15% to 40%.

For large strained samples, the LBs, which are a single extended nearly straight boundary including cell blocks and have larger misorientation angle, could be regarded as GNBs in EBSD maps. In Fig. 5, the boundary ($> 15^\circ$) spacing represents the average intercept of all LBs in the normal direction of the longitudinal side plane. There is a distinct decrease in spacing between LBs with strain increasing from 1.09 to 2.54, and subsequently the spacing gradually reduces and approximates a constant value of $\sim 0.4 \mu\text{m}$ at a strain of 4.52.

3.3 Microtexture evolution

For fcc metals and alloys with medium to high stacking fault energy, a typical cold rolling texture was developed along the β fiber in Euler angle space during deformation [22]. The main three deformation orientations are brass, S and copper. The β fiber is an orientation assemblage which starts from the brass orientation via the S orientation and ends with the copper orientation. EBSD maps of Ni–W substrates with different reduction are shown in Figs. 2 and 3, respectively. In the EBSD maps, different colors were

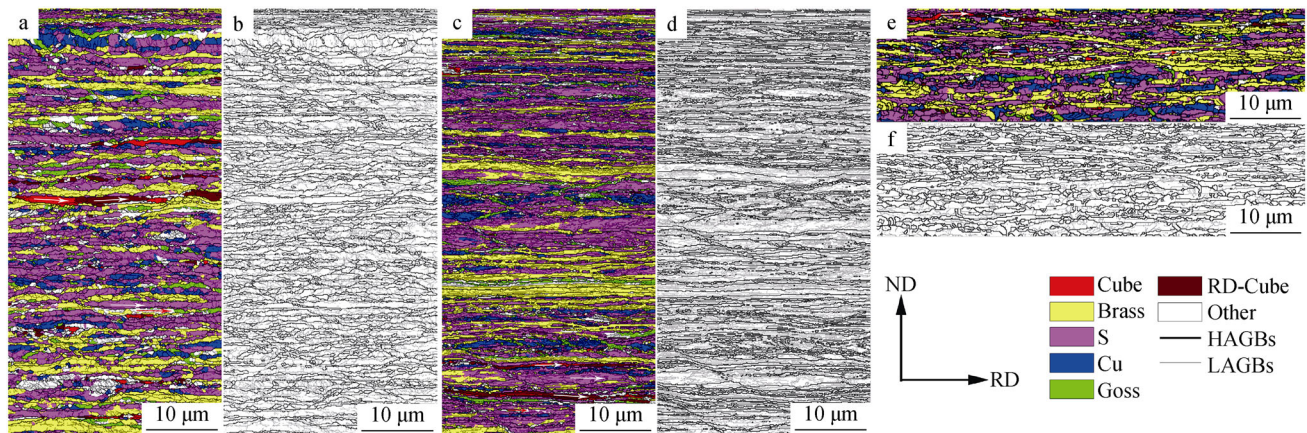


Fig. 3 EBSD maps of Ni–W substrates with 77%, 89% and 98% rolling reductions: **a** 77% OIM, **b** 77% grain boundary map, **c** 89% OIM, **d** 89% grain boundary map, **e** 98% OIM, and **f** 98% grain boundary map

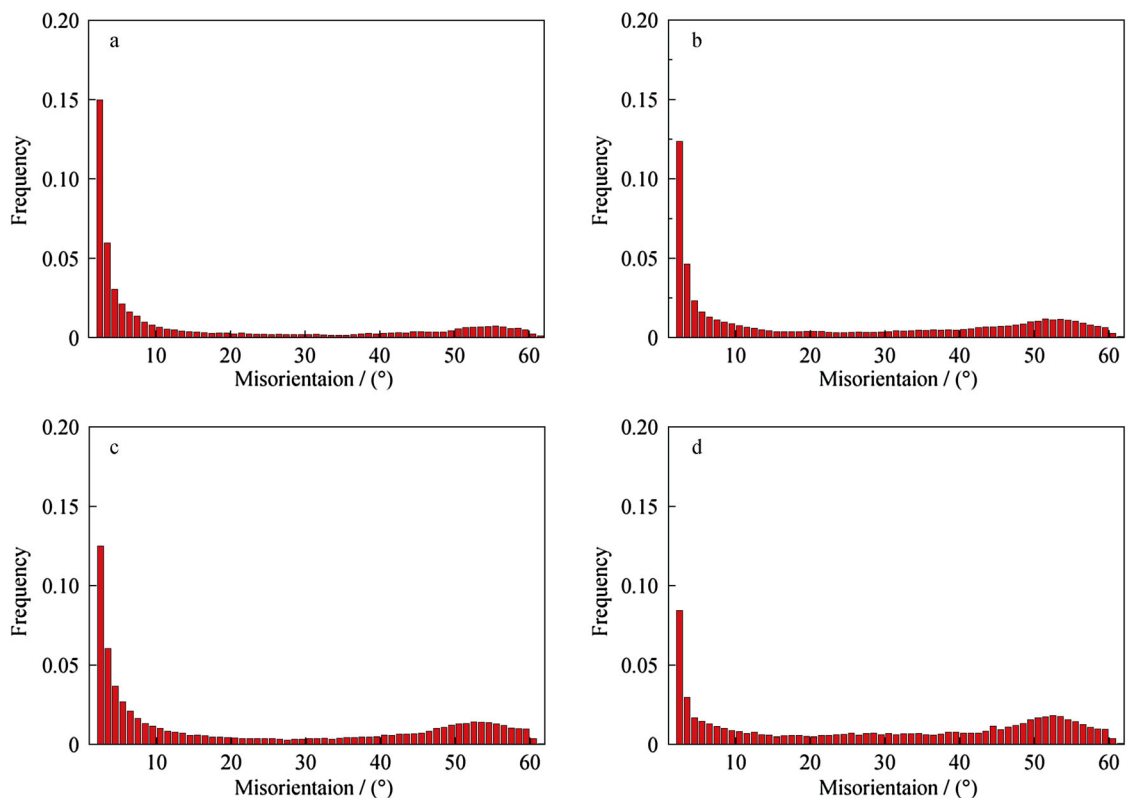


Fig. 4 Grain boundary character distribution of Ni–W substrates for different rolling reductions: **a** 61%, **b** 77%, **c** 89%, and **d** 98%

used to represent different texture components, i.e., S, copper, brass, Goss, cube and the random texture are represented in purple, blue, yellow, green, red and white, respectively. The area fractions of the main texture components which contain S, copper, brass, Goss, cube + RD-rotated cube and other texture (random texture) were calculated from the EBSD maps and plotted as a function of the deformation reduction (Fig. 6). The dominant deformation orientation is S, which is proved by a very high area

fraction of the S component (nearly 50%). The other major components are copper and brass, which have similar area fraction. Also, the area fraction of S component is about two times that of copper or brass. It is seen that the contents of S, copper and brass increase slightly, while random texture orientation shows an apparent decrease. Other rolling texture orientations are present only in minor proportion. It is clear that the rolling texture orientations

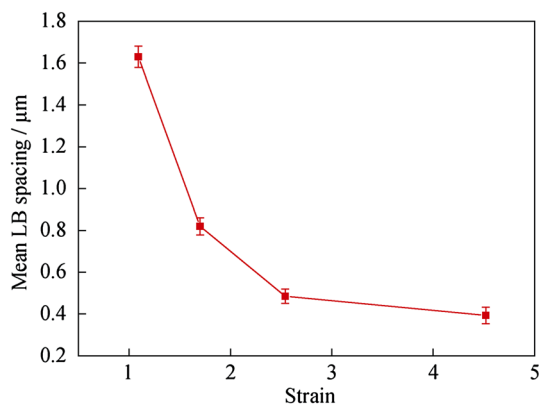


Fig. 5 Development of lamellar boundary ($> 15^\circ$) spacing with deformation strain

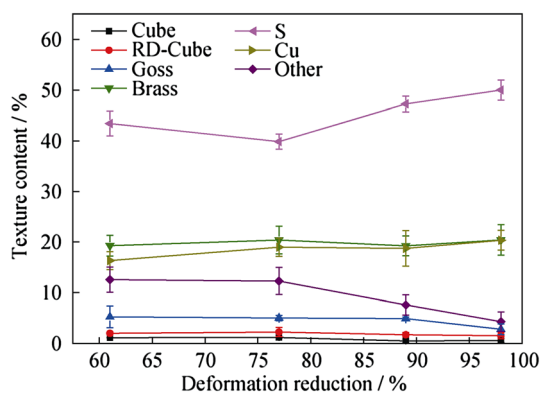


Fig. 6 Texture component evolution as a function of rolling reduction, each data point representing average for three EBSD maps

gradually strengthen with reduction increasing at the expense of random texture orientations.

In addition, it is worth noting that the cube and RD-rotated cube-oriented regions are already present in the intermediate reduction and decrease slowly with the increase in reduction. Even after the highest reduction, cube-oriented region remains. It has been pointed that the preexisting cube-oriented regions in the deformed matrix could result from the remnants of cube-oriented grains in the hot-rolled state [23, 24], or a rotational mechanism [14]. Although the area fraction of these oriented is small, it is supposed that the preexisting cube-oriented regions in the deformed material have a direct relation with the formation of strong cube texture [25].

The recrystallization texture of sample with 98% rolling reduction is shown in Fig. 7. In this map, the color indicates the deviation extent of ideal cube orientation. The recrystallization texture consists primarily of the cube and RD-rotated cube components. The area fraction of the cube and RD-rotated component is found to be about 96% and 48%, respectively. It is worth noticing that there is a large overlap between orientation spreads around the cube and

RD-rotated cube orientations. Furthermore, according to the histogram of grain boundary misorientation (Fig. 7b), the fraction of LAGBs can be calculated as 91%. It could also show that the boundaries with a twin misorientation of 60° are detected and the fraction of this boundary can be neglected ($\sim 2\%$). The sharp cube texture and a small amount of twin can also be seen from the pole figure (Fig. 7c). However, such sharp cube texture could not be obtained with smaller rolling reduction (61%, 77%, 89%) under the same annealing temperature range. This result complies with the former reports [4, 26–28].

4 Discussion

4.1 Microstructure analysis

In the present work, a continuous evolution of the microstructure in Ni–W alloy has been shown in the above results. From an overall perspective, the microstructural evolution gradually generates from MB or plate-like microstructure to LB microstructure in the strain range from intermediated to high. In Fig. 4, HAGBs gradually increase with strain increasing. One of the most significant reasons is that a part of LAGBs, whose misorientations increase slowly with strain, may eventually become HAGBs. For instance, according to the classification in the experimental section, the boundaries which have 10° – 15° misorientations (identified as LAGBs) become HAGBs with strain increasing whose misorientations exceeding 15° . Additionally, a number of HAGBs are created during deformation, maybe also because that individual grains may break into several regions with different texture components, which subdivide the origin grains with HAGBs [29, 30]. The formation of HAGBs is favorable for the nucleation process during annealing treatment, since they meet the criteria and are the potential nucleation locations of recrystallization grains [31]. At large strains, as the grain shape changes from an equated to uneven striped distribution along the rolling direction, the spacing of grain boundaries becomes smaller and the area of grain boundaries also increases. The closer spacing and larger grain boundary area will increase the resistance of dislocation glide. Thus, the boundary spacing is regarded as a characteristic parameter of strength, and it gradually approaches a constant value at large strains.

4.2 Texture analysis

The texture measurement of cold rolling Ni–W alloy shows a typical pure metal or copper-type rolling texture. The fraction of deformation texture increases as the reduction increase from 61% up to 98%. Figure 8 shows the point-to-

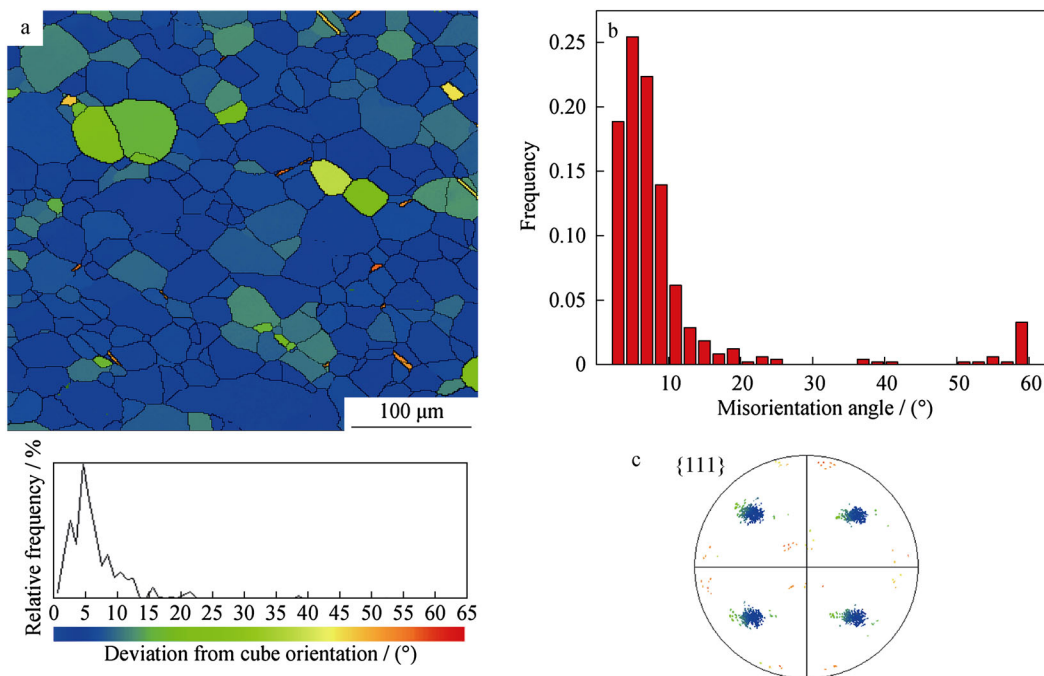


Fig. 7 **a** EBSD map, **b** grain boundary misorientation distribution and **c** {111} pole figure of 98% reduction Ni–W substrates annealed at 1200 °C for 30 min

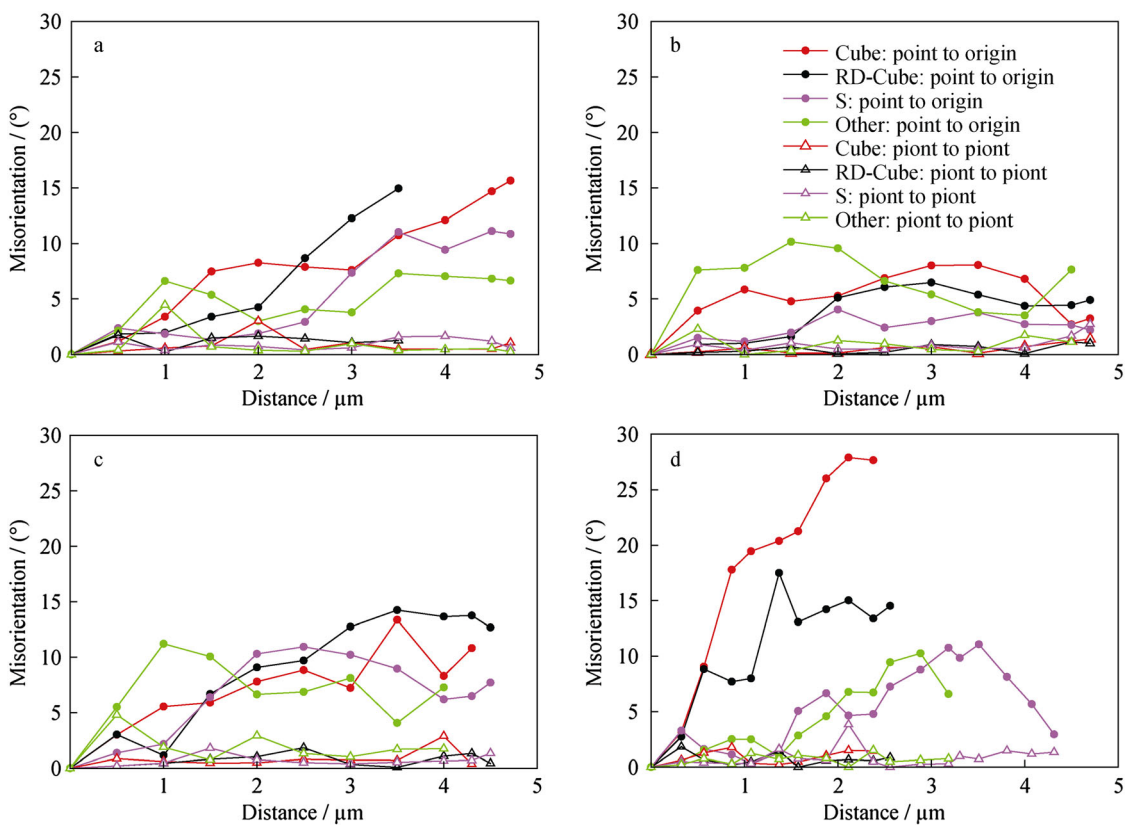


Fig. 8 Evolution of point-to-point and accumulated misorientation at reductions of **a** 61%, **b** 77%, **c** 89%, and **d** 98%

point and point-to-origin misorientations of cube, RD-rotated cube, S and other orientations, as marked by the arrows in EBSD maps in Figs. 2 and 3. The point-to-point misorientations inside all bands are found to be quite low and vary between 1° and 4° . But the point-to-origin misorientations reach a higher value. The accumulated misorientations have no essential difference in cube and non-cube-oriented regions when the reduction is 61%–89%. Therefore, no significant orientation gradient is found for bands of cube orientation. When the deformation reduction reaches up to 98%, however, there is an obvious orientation gradient (close to about 28° in specific condition) extending over the whole cube band compared to non-cube-oriented bands. It may be interesting to note that orientation gradient can be also formed in the RD-rotated cube bands, which is lower than that in cube bands, but has an advantage with respect to other non-cube-oriented bands. As shown in Figs. 2 and 3, cube-oriented-regions appearing in long, thin bands parallel to the RD are found in the deformed state. And the RD-rotated cube regions are always located at the same striped band or adjacent regions with cube band. This indicates that the RD-rotated cube regions are a result of the rotation of cube-oriented-cells around the RD toward the $\{013\} \langle 100 \rangle$ orientation. A slight cell rotation has occurred which will become the RD-rotated cube-oriented region, whereby the region which first began to rotate will eventually be rotated furthest away from the original cubic orientation [32]. Therefore, this rotation of the cube orientation about RD seems to result in a high accumulated orientation gradient inside the cube bands. Similar results have also been mentioned in other studies [14, 32, 33].

In the current case, the high orientation gradients within the cube bands in the 98% deformed Ni–W alloys are highly favorable for the nucleation of cube grains. As shown in Fig. 7, a sharp cube texture is developed in the sample with 98% rolling reduction and subsequent annealing at 1200°C for 30 min. In order to nucleate, the nucleus must meet the following criteria: (1) the nucleus must exceed a critical size; (2) the nucleus should be surrounded by HAGBs with its neighbors. Zaefferer et al. [32] investigated Fe-36 wt% Ni alloy and proposed that the cube nucleus is formed by subgrain growth inside the cube bands with high orientation gradients which easily leads to the formation of HAGBs. Therefore, the nucleation process described in cube bands would be quite rapid than other orientations because HAGBs may be achieved quickly in the high orientation gradient and the well-recovered nature of cube regions [32]. None of these properties are found in other orientation bands. In addition, RD-rotated cube texture also has orientation gradient in the deformed state and appears to be quite strong in recrystallized material (Fig. 7). It seems that RD-rotated cube component has

some effect on the recrystallization texture. This is agreement with the investigation by Bhattacharjee et al. [33]. They also have discussed that the RD-rotated cube component may be nucleating behind the cube grains perhaps due to their different recover/recrystallization kinetics. In the present research, however, the attention was focused on the deformation microstructure, a more detailed analysis of the relation between the formation of the recrystallization cube texture and the cube bands as well as the RD-rotated cube regions should be discussed in the next study.

5 Conclusion

The evolution of microstructure and texture of Ni–5W alloy from medium to high strain was studied in detail. The most important conclusions were summarized. From intermediate to high strain, the microstructure evolves from MB or plate-like microstructure to lamellar microstructure. The microtexture in the cold-rolled condition is a typical pure metal deformation texture. A sharp cube texture is obtained after heavy cold rolling and subsequently annealing at 1200°C for 30 min. In addition, the cube orientation bands are found to be already present in the deformed state, which also have a high orientation gradient compared to non-cube-oriented regions under large enough strain. The prior nucleation of the cube grains may have a very close relationship with the beneficial structure of the cube bands which have a high orientation gradient. In addition, RD-rotated cube component appears to have significant effect on the recrystallization texture.

Acknowledgements This project was financially supported by the National Natural Science Foundation of China (No. 51171215).

References

- [1] Goyal A, Norton DP, Christen DK, Specht ED, Paranthaman M, Kroeger DM, Budai JD, He Q, List FA, Feenstra R, Kerchner HR, Lee DF, Hatfield E, Martin PM, Mathis J, Park C. Epitaxial superconductors on rolling-assisted biaxially-texture substrates (RABiTS): a route towards high critical current density wire. *Appl Supercond.* 1996;4(10):403.
- [2] Goyal A, Norton DP, Budai JD, Paranthaman M, Specht ED, Kroeger DM, Christen DK, He Q, Saffian B, List FA, Lee DF, Martin PM, Klabunde CE, Hartfield E, Sikka VK. High critical current density superconducting tapes by epitaxial deposition of $\text{YBa}_2\text{Cu}_3\text{O}_x$ thick films on biaxially textured metals. *Appl Phys Lett.* 1996;69(12):1795.
- [3] Norton DP, Goyal A, Budai JD, Christen DK, Kroeger DM, Specht ED, He Q, Saffian B, Paranthaman M, Klabunde CE, Lee DF, Sales BC, List FA. Epitaxial $\text{YBa}_2\text{Cu}_3\text{O}_7$ on biaxially textured nickel (001): an approach to superconducting tapes with high critical current density. *Science.* 1996;274(5288):755.

- [4] Chang H, Baker I. Effects of degree of deformation and deformation temperature on primary recrystallization textures in polycrystalline nickel. *Metall Mater Trans A*. 2007;38(11):2815.
- [5] Liu DM, Hao F, Li MJ, Hu YC, Gao F, Zhou ML. Study on texture of Ni–W substrates for high temperature superconductors. *Mater Sci Technol Lond*. 2005;21(12):1387.
- [6] Liu JN, Liu W, Tang GY, Zhu RF. Fabrication of textured Ni–9.3at%W substrate by electropulsing intermediate annealing method. *Phys C Supercond*. 2014;497(2):119.
- [7] Eickemeyer J, Selbmann D, Opitz R, Boer B, Holzapfel B, Schultz L, Miller U. Nickel-refractory metal substrate tapes with high cube texture stability. *Supercond Sci Technol*. 2001;14(3):152.
- [8] Hui T, Suo HL, Qiu HQ, Liu M, Ma L, Wang LM, Yuan DM, Wang YX. Investigation of cold rolling texture and recrystallization texture in NiW substrates. *Rare Met Mater Eng*. 2011;40(3):329.
- [9] Zhao Y, Suo H, Zhu Y, Grivel J, Gao M, Ma L, Fan R, Liu M, Ji Y, Zhou M. Study on the formation of cubic texture in Ni–at% W alloy substrates by powder metallurgy routes. *Acta Mater*. 2009;57(3):773.
- [10] Eickemeyer J, Hühne R, Güth A, Rodig C, Klauß H, Holzapfel B. Textured Ni–7.5 at% W substrate tapes for YBCO-coated conductors. *Supercond Sci Technol*. 2008;21(10):105012.
- [11] Hughes DA, Hansen N. Microstructure and strength of nickel at large strains. *Acta Mater*. 2000;48(3):2985.
- [12] Rosen GI, Jensen DJ, Hughes DA, Hansen N. Microstructure and local crystallography of cold rolled aluminium. *Acta Metall Mater*. 1995;43(7):2563.
- [13] Hughes DA, Hansen N. Microstructural evolution in nickel during rolling and torsion. *Mater Sci Technol Lond*. 1991;7(6):544.
- [14] Bhattacharjee PP, Ray RK, Tsuji N. Cold rolling and recrystallization textures of a Ni–5 at% W alloy. *Acta Mater*. 2009;57(7):2166.
- [15] Gao MM, Grivel JC, Suo HL, Zhao Y, He D, Andersen NH. Fabrication of a textured non-magnetic Ni–12 at% V alloy substrate for coated conductors. *IEEE Trans Appl Supercond*. 2011;21(3):2973.
- [16] Bhattacharjee PP, Ray RK. Effect of processing variables on cube texture formation in powder metallurgically prepared Ni and Ni–W alloy tapes for use as substrates for coated conductor applications. *Mater Sci Eng A Struct*. 2007;459(1):309.
- [17] Humphreys FJ. Review-grain and subgrain characterization by electron back scatter diffraction. *J Mater Sci*. 2001;36(16):3833.
- [18] Soubeyroux JL, Bruzek CE, Girard A, Jorda JL. Thermal treatments for biaxially textured Cu–Ni alloys for YBCO coated conductors. *IEEE Trans Appl Supercond*. 2005;15(2):2687.
- [19] Tian H, Suo HL, Wulff AC, Grivel JC, Mishin OV, Jensen DJ. Comparative characterization of Cu–Ni substrates for coated conductors. *J Alloys Compd*. 2014;601(7):9.
- [20] Vadlamani SS, Eickemeyer J, Schultz L, Holzapfel B. Rolling and recrystallisation textures in Cu–Al, Cu–Mn and Cu–Ni alloys. *J Mater Sci*. 2007;42(17):7586.
- [21] Hughes DA, Hansen N. Microstructural evolution in nickel during rolling from intermediate to large strains. *Metall Trans A*. 1993;24(9):2021.
- [22] Sarma VS, Eickemeyer J, Mickel C, Schultz L, Holzapfel B. On the cold rolling textures in some fcc Ni–W alloys. *Mater Sci Eng A Struct*. 2004;380(1):30.
- [23] Vatne HE, Shahani R, Nes E. Deformation of cube-oriented grains and formation of recrystallized cube grains in a hot deformed commercial AlMgMn aluminium alloy. *Acta Metall Mater*. 1996;44(11):4447.
- [24] Vatne HE, Furu T, Nes E. Nucleation of recrystallised grains from cube bands in hot deformed commercial purity aluminium. *Mater Sci Technol Lond*. 1996;12(3):201.
- [25] Cheng Z, Godfrey A, Zhang YB, Liu W, Liu Q. The influence of pre-annealing on recrystallization in heavily cold-rolled nickel. *Key Eng Mater*. 2007;353(1):703.
- [26] Li LF, Chen XP, Sun HF, Li XG. Effect of strain on grain boundary character distribution in Ni–5 at% W alloy. *Trans Mater Heat Treat*. 2015;36(6):26.
- [27] Chang H, Baker I. Isothermal annealing of cold-rolled high-purity nickel. *Mater Sci Eng A Struct*. 2008;476(1–2):46.
- [28] Liu ZY, Li WF, Zhang N, Yang F, Song GL, An YP, Zhang H, Chang FG. Fabrication and properties of non-magnetic strong cube textured Cu₆₀Ni₄₀ alloy substrate. *Rare Met Mater Eng*. 2015;44(9):2295.
- [29] Hughes DA, Hansen N. High angle boundaries formed by grain subdivision mechanisms. *Acta Mater*. 1997;45(9):3871.
- [30] Hughes DA, Hansen N. High angle boundaries and orientation distributions at large strains. *Scr Metall Mater*. 1995;33(2):315.
- [31] Doherty RD, Hughes DA, Humphreys FJ, Jonas JJ, Jensen DJ, Kassner ME, King WE, McNelley TR, McQueen HJ, Rollett AD. Current issues in recrystallization: a review. *Mater Sci Eng A Struct*. 1997;238(2):219.
- [32] Zaefferer S, Baudin T, Penelle R. A study on the formation mechanisms of the cube recrystallization texture in cold rolled Fe–36% Ni alloys. *Acta Mater*. 2001;49(6):1105.
- [33] Bhattacharjee PP, Ray RK, Tsuji N. Evolution of deformation and recrystallization textures in high-purity Ni and the Ni-5 at. pct W alloy. *Metall Trans A*. 2010;41(11):2856.